Flexural properties of a composite geofoam-geogrid material for use in embankments on polygonal ground

Earl Marvin De Guzman & Marolo Alfaro
Department of Civil Engineering, University of Manitoba, Canada

ABSTRACT: Most road embankments in northern Canada are being built on permafrost terrain on thaw sensitive foundations. Permafrost degradation and thawing of ice wedges (polygonal ground) can cause excessive differential deformations and embankment failures caused by sinkholes resulting in significant maintenance efforts and safety hazards. The flexural properties of a composite geofoam-geogrid material known as Reinforced Polymer Base® (RPB) were investigated in the laboratory by performing bending tests. Results from laboratory tests will help assess the effectiveness of the composite material as reinforcement of road or railway embankments on polygonal ground and how the design and construction of embankments with RPB can be designed in the future.

Keywords: composite geofoam-geogrid, compression testing, flexural testing, embankments

1 INTRODUCTION

Most road embankments in Northern Canada are being built on permafrost terrain on thaw sensitive foundations. Some of these roads traverse polygonal-pattern ground containing ice wedges (shown in Figure 1a). Permafrost degradation and thawing of ice wedges can cause excessive differential deformations, instabilities of the embankment, or complete embankment failure caused by sinkholes resulting to significant maintenance costs and safety hazards (Figure 1b). There is no record of the performance of a Reinforced Polymer Base (RPB) in cold region applications. There are also no available design guidelines for such applications. Research is needed in the form of laboratory tests to determine the mechanical and thermal characteristics of RPB including its interaction with the soil. Design parameters should be determined under field environmental conditions including the effects of freeze-thaw cycles. Results from laboratory tests will help assess the effectiveness of RPB as base insulator and reinforcement of road or railway embankments on polygonal ground and how embankments with RPB can be designed in the future.

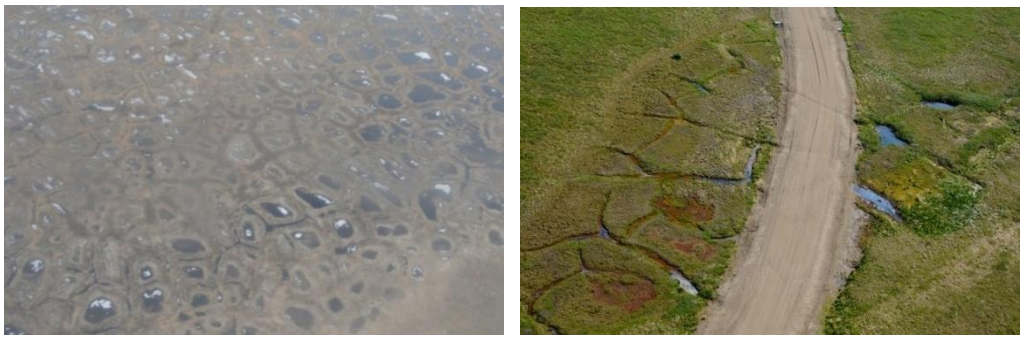

(a) (b)

Figure 1. Examples of permafrost terrain: (a) Polygonal pattern ground with ice wedges and (b) a highway section crossing ice wedges (courtesy of Don Haley)

A series of laboratory tests were conducted in the Geotechnical Laboratory at the University of Manitoba to determine the design properties for the RPB material manufactured by Poly-Mor. The potential failure mechanisms involved in assessing the strength and performance of the RPB were investigated, specifically its behaviour in flexure. The flexural properties of the RPB, hereto referred to as 'foam', are essential in determining its load carrying capacity. The flexural properties of the foam are hypothesized to be affected by the water absorbed by the material, the temperature at the time of testing, and freeze-thaw cycling. The flexural properties of the foam can be used to calculate the settlements as voids develop under it and minimize the differential settlement at the embankment surface (Figure 2). The flexural properties of the foam based on a series of four-point bending tests under different testing conditions are presented in this paper. Preliminary numerical deformation models using the properties obtained are also presented.

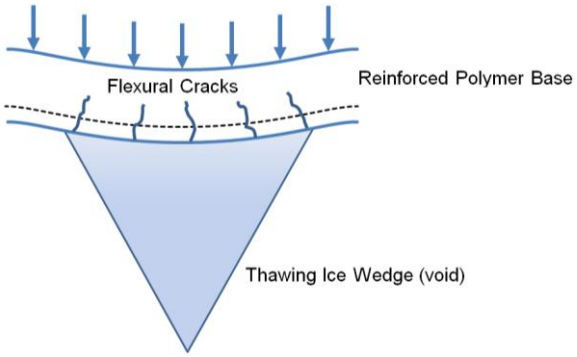

Figure 2. Conceptual behaviour of foam in flexure

2 METHODOLOGY

Beams were formed in a formwork of dimensions 900 x 150 x 150 mm (L x W x H) with the geogrid positioned at a distance of 30 mm from the base of formwork. Aluminum ties were used to anchor the centre part of the geogrid to account for the expansion of the foam during spraying. Additional tension was applied to the geogrid by using shims on both ends of the formwork. Two geogrid configurations were tested: a bigger aperture and the original aperture. The purpose of the modified dimensions of the geogrid is to investigate the effect of aperture size with respect to the load-carrying capacity of the beam. Saturated samples were submerged in water with a head of 1 in. above the top of the beam (Figure 3a). Samples are left to saturate for a period of 7, 11, and 15 days before testing (ASTM C1763, 2012). Samples tested at freezing conditions were conditioned in a chest freezer at -20^{o}C for 6 days before testing. Cycling of samples were done by taking the samples in and out of the chest freezer for a period of 24 hours for each cycle for 6 days. After conditioning (saturation, freezing, cycling), beam samples were tested in a four-point bending test frame (Figure 3b) as per ASTM C 203-5a (2012).

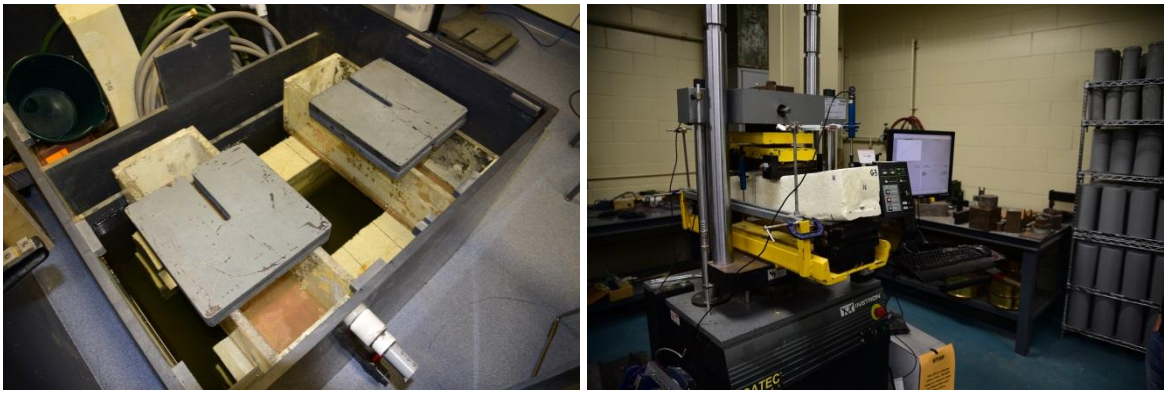

(a) (b)

Figure 3. (a) Beam sample saturation and (b) four-point beam testing frame

Three displacement transducers were placed on the sample: two at the supports and one at the middle of the beam. Distance between supports is at 765 mm, with loading points at the top of the beam with a distance of 255 mm (L/3) from each support. Displacements and loads are recorded and saved in a data

acquisition system. Samples with deformities (Figure 4) are discarded from the testing program. Table 1 shows the sample matrix for the testing program. Three samples were tested in each condition but test results that showed significantly different results were removed from the analysis. Actual number of samples included in the analysis is provided in Table 2.

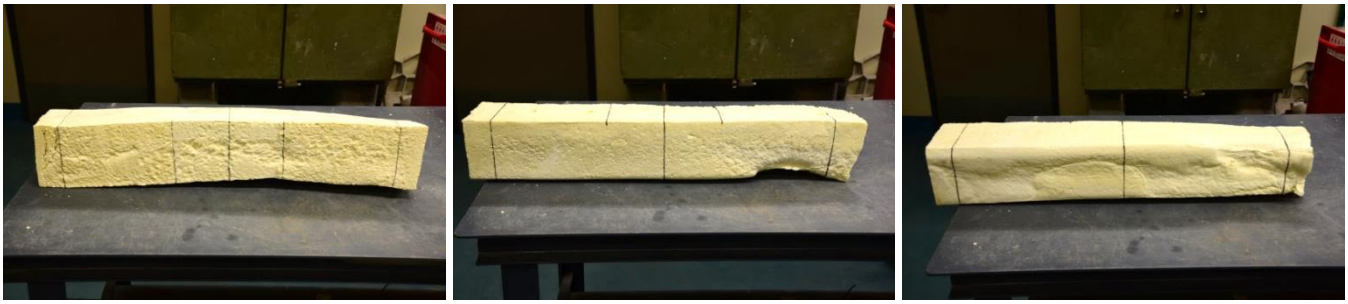

(a) (b) (c)

Figure 4. Beam samples rejected for flexural testing due to deformities

Table 1. Sample matrix for bending tests under different conditions

Freeze-Thaw Cycling	Saturation Condition	Reinforcement (aperture size)	Testing Temperature	
			-20°C Sample Label	+20°C Sample Label
Without cycling	As prepared	Bigger Aperture	G (3)[1]	A (3)
		Original Aperture	H (3)	B (3)
	Fully saturated	Bigger Aperture	J (3)	D (3)
		Original Aperture	K (3)	E (2)
Without cycling	As prepared	Unreinforced	I (2)	C (3)
	Fully saturated	Unreinforced	L (2)	F (2)
With cycling	Fully saturated	Bigger Aperture		M (3)
		Original Aperture		N (3)
		Unreinforced		O (3)

[1] Number in parentheses indicates number of samples tested in that condition

3 FLEXURAL STRENGTH

3.1 *Normal and saturated densities*

Table 2 shows the average normal and saturated densities of the beam samples tested as well as the water absorption by volume after saturation. These values were recorded before testing. Dry unit weights for the samples are ranging from 40 to 48 kg/m^3. Beam samples with geogrids (both bigger and original aperture) have higher absorption by volume values compared to unreinforced beam specimens. This can be attributed to the presence of voids close to aperture of the geogrid, compared to unreinforced samples where the whole void is occupied. The difference in absorptions can also be attributed to change of the dry densities which are greatly influenced by the resin mixture and setting properties of the foam during spraying. The locations of the geogrids are also summarized in Table 2. The geogrids are located within the range of 26 to 32 mm from the base of the beam samples, whereas the original target is at 30 mm. There is no existing standard or available literature as to where the geogrid should be located and how it affects the load carrying capacity of the beam. The experimental results obtained from this study will be used in numerical modelling for future research to provide a baseline study to optimize the location of the geogrid where it would provide the most benefit.

3.2 *Stress-strain behaviour and modulus of elasticity*

Loads are recorded by a load cell attached to the test frame while the displacement transducers measure the deformation at the centreline of the beam. The loads are converted to moments (Eq. 1) and the results are used to obtain the flexural stresses (Eq. 2). The average height and width of the specimen at the centreline of the beam was used to derive the moment of inertia in Eq. 2. It was assumed that the area occu-

pied by the geogrid is negligible. The modulus of elasticity was obtained using Eq. 3. The modulus of elasticity varies as the beam bends (v is the displacement at the centreline). Assuming that the centreline section of the beam remains in the same plane after bending, Hooke's Law was used to derive the bending strains at the bottom of the beam.

$$M_{centreline} = PL / 6 \quad (1)$$

where $M_{centreline}$ is the moment at the centreline of the beam, P is load recorded by the load cell, and L is the centre-to-centre distance between the support ends of the test frame.

$$\sigma = M_{centreline} / S \quad (2)$$

where S is the section modulus (S = I / y), y is the location of the outermost fibre from the centroid of the cross-section at midspan, and I is the moment of inertia of the cross-section at midspan.

$$E = PL^3 / 48Iv \quad (3)$$

where v is the displacement at the centreline.

Table 2. Summary of densities and geogrid locations for beam samples

Sample Label	Dry Unit Weight (kg/m^3)	Days under saturation	Saturated Unit Weight (kg/m^3)	Absorption by Volume (%)	Geogrid location from base (mm)
A	45.02				31
B	45.15				27
C	44.22				
D	45.78	11	75.99	3.02	30
E	45.70	11	71.46	2.58	26
F	44.12	7	57.66	1.35	
G	45.56				30
H	44.87				29
I	43.55				
J	45.47	7	69.27	2.38	28
K	46.68	7	76.65	3.00	27
L	41.76	7	53.90	1.21	
M	45.13	15	74.50	2.94	32
N	47.98	15	91.67	4.37	28
O	40.87	11	54.76	1.39	

The flexural stresses and modulus of elasticities versus strain plots for each condition tested are provided in Figures 5 to 9. The results of each test set (e.g. 3 samples for set A) with respect to the effect of the geogrid are shown. For clarity in presenting the results, a parabolic function was used to fit the data for the response at each condition for the stress-strain plots. A linear function was used for the modulus of elasticity on a semi-logarithmic scale.

It can be noticed in Figure 5 that the effect of the geogrid, both bigger and original aperture, did not contribute to the increase in strength for the condition where samples were tested under room conditions with no saturation at all. This is probably due to the insufficient bonding of the foam to the geogrid for both cases or the formation of voids just above the geogrid during foaming. There is not much difference in the stress-strain relationship between the two apertures. The modulus of elasticity for the unreinforced beams shows slightly higher values compared to the reinforced ones. The saturated samples at room testing conditions (Figure 6) do not show any significant increase in behaviour compared to the as prepared samples (Figure 5). If used in applications where seasonal freezing-thawing is not a concern, saturation of the foam will not cause any deterioration in its flexural strength.

The reinforced samples tested at -20°C (Figures 7 and 8) show an appreciable increase in load-carrying capacity compared to those beams tested at room conditions, but the loads carried in the unreinforced beams are lower compared to those beams tested at 20°C. The saturated samples tested at -20°C (Figure 8) shows slightly higher response in loads at higher strains compared to as prepared samples. The moduli of elasticities are also consistently higher than that of the unreinforced ones for both as prepared and saturated conditions at -20°C. The effect of temperature may have stiffened both the foam and the geogrid providing some additional load-carrying capacity even at higher strains. This behaviour is significant in embankment applications because the reinforced foam with its thermal properties can preserve the cold temperature in the foundation soil. It will retain the cold temperature and maintain higher stiffness and stronger foundation. Thawing generally starts at the toe of the embankment and the water accumulated at the may saturate the beam as well. As indicated in these preliminary results at cold temperature conditions a saturated beam (from spring thawing to winter freeze-up) will have a higher load-carrying capacity. This water would most likely be retained in the pores of the foam. Samples were also tested under cycling conditions (saturated first, frozen, thawed, then tested). Figure 9 shows that the response is almost the same as if the sample was tested as a saturated specimen under room conditions. These results are used in a simple numerical model to show how the foam can be used in the field testing program.

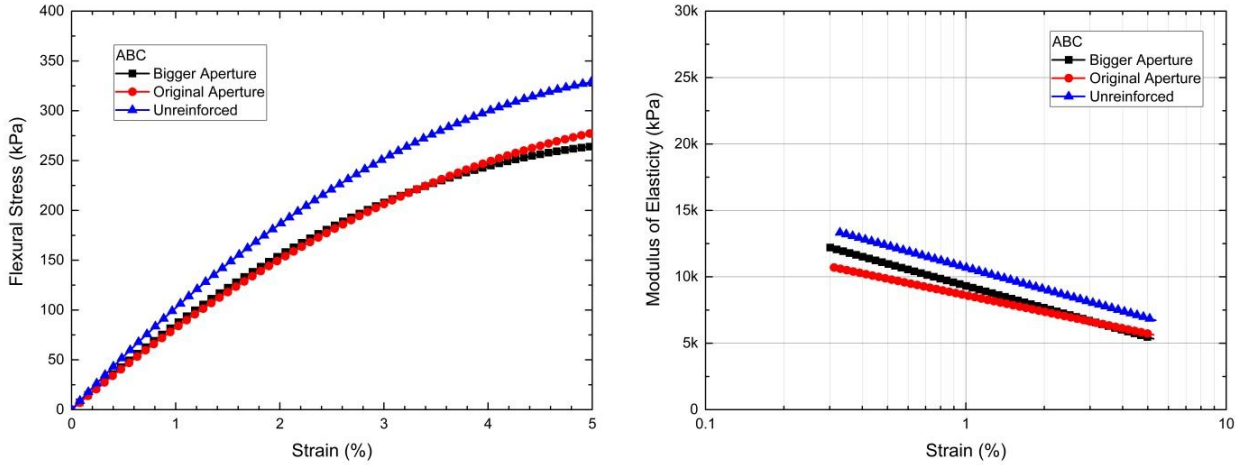

(a) (b)

Figure 5. Comparison of fitted results between test sets A, B, and C with respect to addition of geogrids: (a) flexural stress vs. strain and (b) modulus of elasticity vs. strain

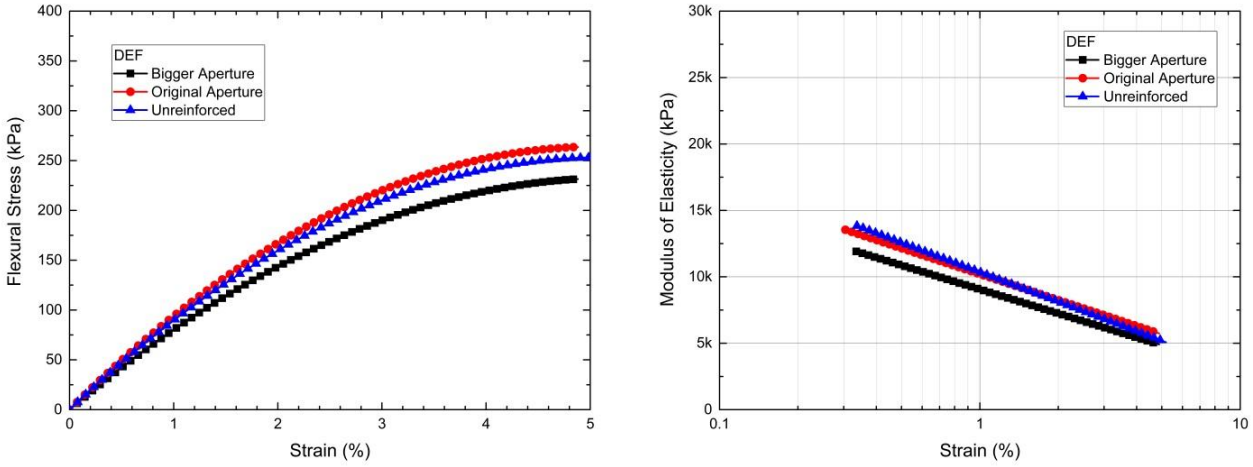

(a) (b)

Figure 6. Comparison of fitted results between test sets D, E, and F with respect to addition of geogrids: (a) flexural stress vs. strain and (b) modulus of elasticity vs. strain

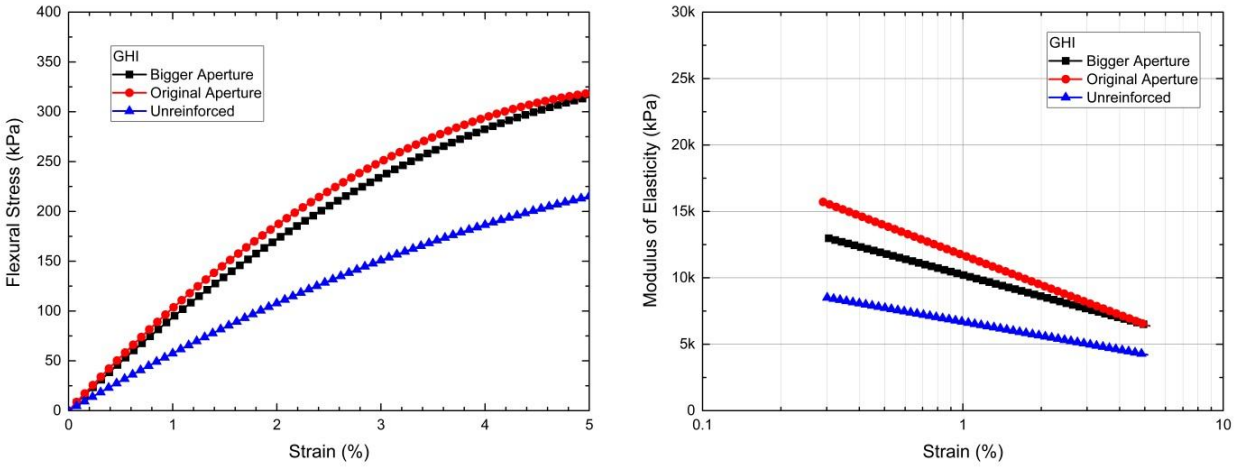

(a) (b)

Figure 7. Comparison of fitted results between test sets G, H, and I with respect to addition of geogrids: (a) flexural stress vs. strain and (b) modulus of elasticity vs. strain

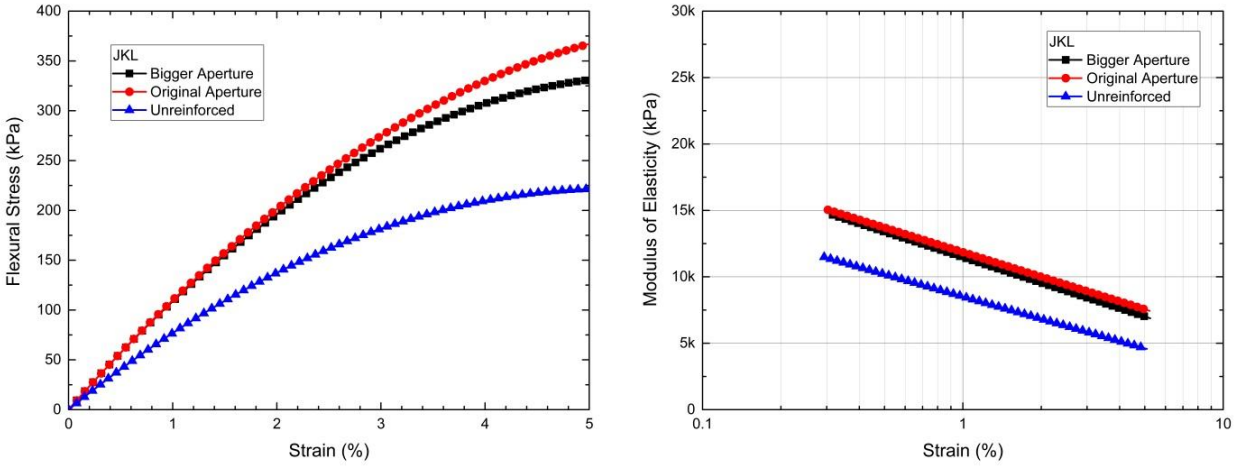

(a) (b)

Figure 8. Comparison of fitted results between test sets J, K, and L with respect to addition of geogrids: (a) flexural stress vs. strain and (b) modulus of elasticity vs. strain

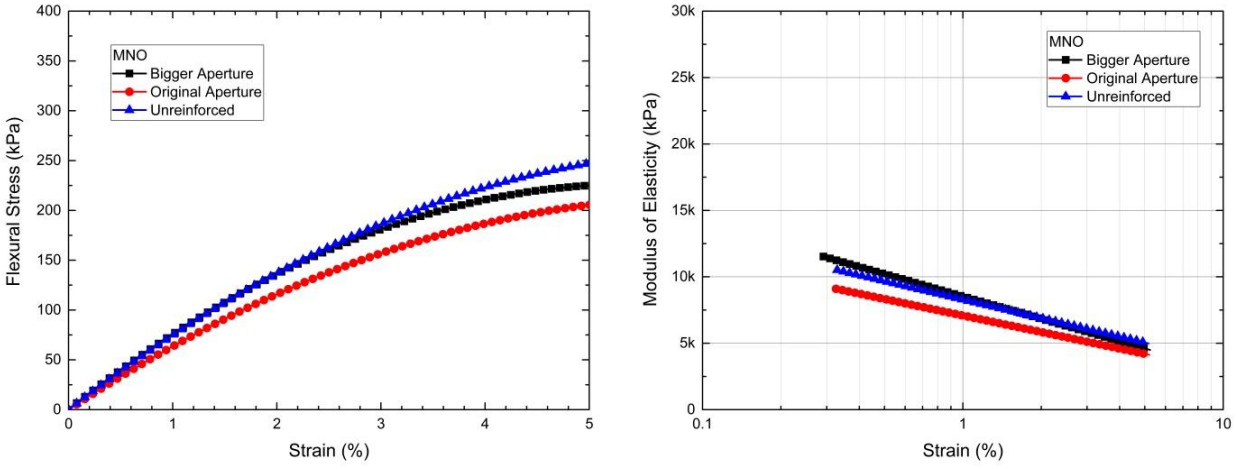

(a) (b)

Figure 9. Comparison of fitted results between test sets M, N, and O with respect to addition of geogrids: (a) flexural stress vs. strain and (b) modulus of elasticity vs. strain

4 SAMPLE APPLICATION ON THE USE OF FLEXURAL PROPERTIES

Results obtained from the flexural testing program are used in a simple numerical model in SIGMA/W (Geo-Slope International 2007) to understand how the foam will support the embankment once the void develops, specifically how the settlements will propagate to the road surface. Figure 10 shows two sketches of an embankment where the foam is added at the base of the embankment. The foam was modelled both as a structural beam carrying the flexural properties and a substitute soil material for its compression properties. These properties along with the other mechanical properties that will be investigated in the future (shear properties of the foam, pullout properties of the geogrid) will be used in advanced finite element software to understand the full interaction between the embankment, the foam, and foundation to evaluate its long-term performance.

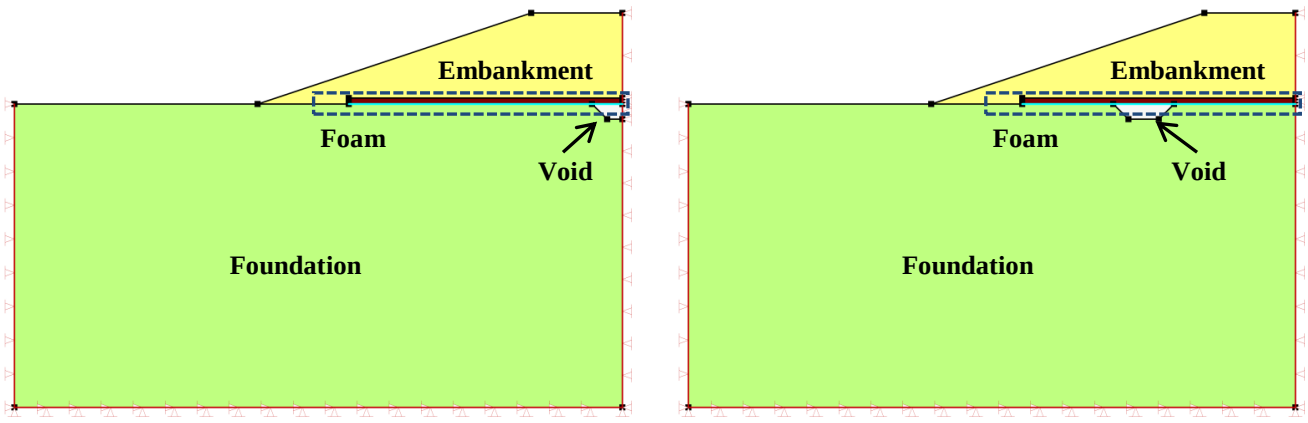

(a) (b)

Figure 10. SIGMA/W models for void development in the foundation soil:
(a) centreline void and (b) offset void

The material properties used for the embankment and foundation soil are summarized in Table 3. The embankment has a height of 3 m, with a road width of 3 m and slopes of 3H:1V. Only half of the embankment is modelled because of symmetry. The structural beam has an E = 7000 kPa, A = 0.15 m^2, and I = 0.0125 m^4. The substitute soil has an E = 11000 kPa and γ = 0.7 kN/m^3 for the compression properties. The numerical model was developed under plane strain conditions. The full height of the embankment was constructed on top of the foundation soil to establish the initial stresses before development of voids. To understand how the foam behaves when the voids develop, a region underneath the centreline and shoulder of the embankment in the foundation soil was removed. A similar model without the foam was analyzed to see how the settlements are reduced along the base of the embankment with the presence of foam.

Table 3. Soil properties for SIGMA/W

Soil	Material Model	Modulus of Elasticity	Cohesion	Friction Angle	Unit Weight
Embankment	Elastic-Plastic	30000 kPa	5 kPa	30^o	18 kN/m^3
Foundation	Elastic-Plastic	25000 kPa	5 kPa	28^o	18 kN/m^3

Figure 11 shows the results of the numerical models with respect to the settlements along the base of the embankment with both centreline and offset voids in the embankment. T1 indicates the void with opening of 1 m (half of the full model) at the centreline, while T2 indicates the void with opening of 2 m at an offset. The depth of the opening is 0.5 m for both cases. In the case of T1, the initial displacement was about a maximum of 135 mm if no foam is present along the base of the embankment. This would translate to a displacement of 84 mm at the top of the embankment. When the foam was added, the resulting displacement was then limited to 33 mm at the centreline of the opening and 26 mm at the top. For T2, the maximum displacement was about 122 mm if no foam is present along the base of the embankment. This would translate to a displacement of 38 mm at the top of the embankment. When the foam was added, the resulting displacement was then limited to 14 mm at the centreline of the opening and 16 mm at the top. It is noteworthy to mention that the settlement behaviour is also a function of the width of the

void opening as well as its depth. The interface properties between the foam the soil have not been investigated in this paper as these properties are still to be obtained in the laboratory. Further studies will be conducted to optimize the design approach and location of the foam in the embankment considering the mechanical properties mentioned earlier.

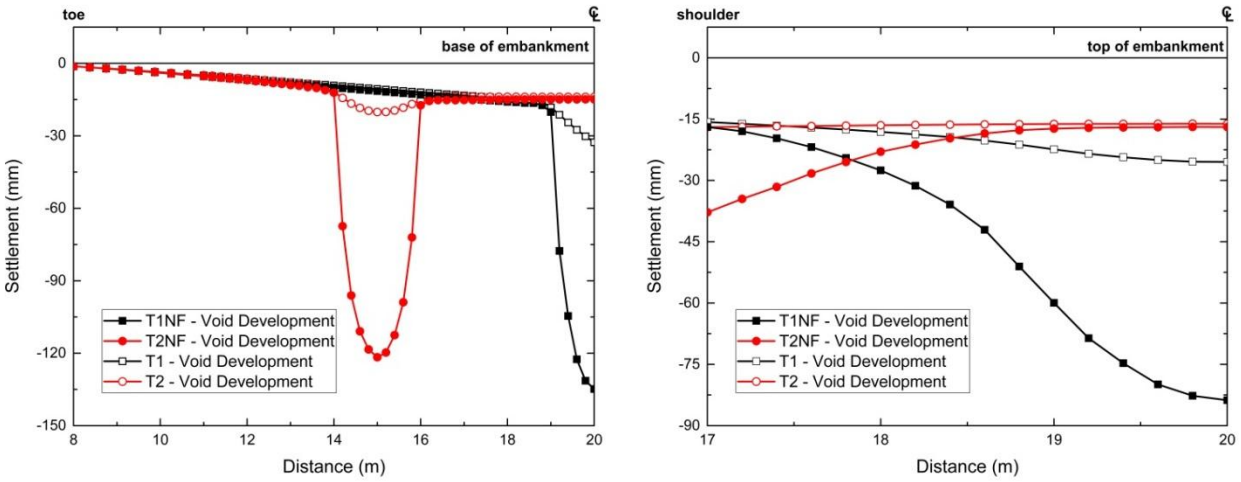

(a) (b)

Figure 11. Settlements (a) along the base and (b) top of the embankment with and without the foam

5 SUMMARY

A series of flexural tests have been conducted on RPB material to determine its flexural properties. The foam material has been subjected to freeze-thaw cycling, saturation, and sub-zero temperatures during the tests to determine the stress-strain relationships and modulus of elasticities for these conditions. Flexural tests were done on reinforced and unreinforced samples, with the reinforced samples having both bigger and original apertures. It was found that the benefit of the geogrid is utilized when it is placed closer to the base of the beam. At the onset of cracking of the foam, the geogrid is expected to sustain the loads from the embankment. A series of fitting functions were developed to characterize the behaviour of the beam and it was found that the environmental conditions where the beams were subjected to affects its behaviour. Care should be exercised when selecting parameters based on these tests. The resin mixture and setting properties of the foam during spraying also affects the compression and thermal properties of the foam and will be investigated in the future.

A numerical model was developed to investigate the behaviour of the foam when it is used in an embankment when a void develops underneath it. It was found that the foam would be able to decrease the settlements and sustain the load imposed by the embankment if the void develops. The contribution of the foam to reduce settlements was found to be both a function of the width and depth of the. Although the numerical models developed are simple, it had provided an insight as to how the embankment might behave and what other design parameters should be investigated to fully utilize the technology. The numerical model has its own limitations and further advancements to it are currently being investigated.

REFERENCES

ASTM C 203-05a. 2012. Standard Test Methods for Breaking Load and Flexural Properties of Block-Type Thermal Insulation, ASTM International, West Conshohocken, PA, DOI: 10.1520/C0203-05AR12, www.astm.org.

ASTM C 1763. 2014. Standard Test Method for Water Absorption by Immersion of Thermal Insulation Materials, ASTM International, West Conshohocken, PA, DOI: 10.1520/C1763-16, www.astm.org.

Geo-Slope International Ltd. 2007. Stress-Deformation Modeling with SIGMA/W 2007. Geo-Slope International Ltd. Calgary, Alberta, Canada.